

## *In silico* estrogen-like activity and *in vivo* osteoclastogenesis inhibitory effect of *Cicer arietinum* extract

Amany A. Sayed<sup>1\*</sup>, Abdo A. Elfiky<sup>2,3,4</sup><sup>1</sup>Zoology Department, Faculty of Science, Cairo University, Giza, Egypt<sup>2</sup>Biophysics Department, Faculty of Science, Cairo University Giza, Egypt<sup>3</sup>Quantitative Life Sciences Section, The Abdus Salam International Center for Theoretical Physics (ICTP), Trieste, Italy<sup>4</sup>Faculty of Pharmacy and Pharmaceutical Sciences, University of Alberta, Edmonton, AB, CanadaCorrespondence to: [amanyasayed@sci.cu.edu.eg](mailto:amanyasayed@sci.cu.edu.eg)

Received October 2, 2017; Accepted April 15, 2018; Published April 30, 2018

Doi: <http://dx.doi.org/10.14715/cmb/2018.64.5.5>

Copyright: © 2018 by the C.M.B. Association. All rights reserved.

**Abstract:** Postmenopausal osteoporosis is a common disorder accompanied with estrogen deficiency in women. Plants containing phytoestrogens and amino acids have been used in the osteoporosis treatment. The present study aims to evaluate the estrogen-like activity of the *Cicer arietinum* extract (CAE) and its ability to inhibit osteoclastogenesis process. These achieved by investigating the binding of its active phytoestrogens (genistein, daidzein, formononetin and biochanin A) to the estrogen receptors (ER)  $\alpha$  and  $\beta$  of rats and human *in silico*. In addition, *in vivo* study on ovariectomized (OVX) rats is performed. For *in vivo* study, twenty four rats were divided into four groups (n= 6). Group I is the sham control rats which administered distilled water. Groups II, III, and IV are OVX groups which administered distilled water, CAE (500 mg/kg), and alendronate; respectively. The docking study revealed that the phytoestrogens docked into the protein active site with binding energies comparable with that of estrogens (estriol and  $\beta$ -estradiol) which means the similarity between the estrogenic contents of CAE and the endogenous ones. Additionally, *in vivo* study revealed that CAE reverse TRAP5b and RANKL levels that drastically increased in the untreated OVX group. But, it trigger upregulation of OPG, enhance the OPG/RANKL ratio and modulate the bone and uterus alterations of OVX group. Phytoestrogens and the bone-protective amino acids contents of CAE could be responsible for their estrogen-like effect and antiosteoporotic activity. These results concluded that CAE is an attractive candidate for developing a potential therapeutic cheap agent used as an alternative to the synthetic estrogen replacement therapy. Further, *in vivo* validation is required for its clinical application.

**Key words:** Estrogen replacement therapy; *Cicer arietinum*; Ovariectomy; Molecular docking.

### Introduction

Postmenopausal osteoporosis is the most common osteoporosis type which become a major problem with significant morbidity and mortality (1). Where reduction of estrogen increases osteolysis rather than osteogenesis; and consequently induces osteoporosis. Both trabecular and cortical bones are affected by postmenopausal osteoporosis (2).

Osteoblasts regulate osteoclast activity via cell-cell contact whereby the osteoblast cell-surface receptor activator of nuclear factor  $\kappa$ -B ligand (RANKL) binds to its cognate receptor (RANK). This results in activation of signaling pathways which regulating osteoclast function; as RANKL is a key promoting factor for osteoclast differentiation. Osteoprotegerin (OPG) expressed by osteoblasts and functions as a soluble decoy receptor for RANKL, it competes with RANK to prevent osteoclastogenesis induction (3). This interaction (OPG with RANK) inhibits osteoclast differentiation consequently prevents bone resorption, thereby is named osteoprotegerin that means "to protect bone" (4). Hence, the osteoclastogenesis activation mainly depends on the ratio of OPG/RANKL specifically generated in the bone microenvironment. As the serum RANKL concentration

does not indicate the bone tissue only due to a variety of cell types express RANKL (5,6). Rogers and Eastell (7) reported that the serological evaluation of OPG is not feasible in all cases because it is possible for the OPG in serum to be linked to another plasma protein and hence become inactive. Thereby, the researchers should be estimate the RANKL and OPG in bone instead of serum. Tanaka et al. (8) considered the RANK/RANKL/OPG axis to be the most relevant therapeutic target for bone destructive diseases. Thus, the search for new regulators for its signaling pathway is considered as a key strategy for bone loss control.

There is an urgent requirement to explore naturally occurring substances especially of plant origin that could prevent bone loss and free from any adverse effects of estrogen replacement therapy and bisphosphonates drugs. Therefore, it would be of great benefit to postmenopausal women to develop plant-derived compounds with estrogenic effects which called phytoestrogens. As the phytoestrogens elicit an estrogenic response by binding with estrogen receptors (ERs). Besides the phytoestrogen importance for the postmenopausal women, proteins represent a key nutrient for bone health and osteoporosis prevention (9). Previous studies reported that proteins of vegetable source increased the bone mineral

density in women, as the amino acids modulate the differentiation of osteoblasts (10,11). Thereby, the ongoing study selects chickpea due to its phytoestrogen contents and its higher protein contents in comparison with the other pulses (12-15). Chickpea (*Cicer arietinum* L.) is the third most important pulse crop in production and has a diverse array of potential nutritional and health benefits.

Molecular modeling represents a new area of research that investigate and examine the physical properties and vibrational characteristics of molecules using the great improvements in software and hardware in the last two decades. New drugs are fabricated nowadays using computer-aided drug design as the first step (16-19). Also, computer simulation of the reactivity and stability of compounds are used to explore molecules before experimental work. The quantitative structure-activity relationships (QSAR) and molecular docking methods performed in the present investigation to study drug-protein interactions and score the reactivity of compounds docked into the protein active site (16,17). The fitting of the drug-like compounds to the protein active/binding site depends on the interaction forces between their atoms. H-bond, Van der Waal's interactions, Columb forces between charges, and ring stacking in aromatic components are the main driving forces that direct the drug-like molecule to the protein's binding site. In addition, water molecules and ions present in the binding site may facilitate ligand binding through H-bond and coordination bonds. Scoring functions test different orientations of the ligand inside the binding cavity and the lowest energy conformation is suggested to be the orientation of choice. The flexibility of side chains and the drug-like molecules represents a favorable choice to mimic the molecular structures at physiological temperature.

Thus, the present study analyze the amino acids of the *Cicer arietinum* extract (CAE) and investigates the pre-clinical osteoclastogenesis inhibitory effect of CAE against estrogen-deficiency bone loss by examining the structural and biochemical properties of bones. Additionally, the current study give the insight view on the bone OPG/RANKL ratio. Further, the present investigation examine and analyze the histomorphometry of the uterus to determine if the CAE has an *in vivo* estrogenic activity or not. Moreover, the reactivity and the binding property of phytoestrogens content (genistein, daidzein, formononetin and biochanin A) of CAE to the rat and human ER $\alpha$  and ER $\beta$  was tested *in silico* using molecular docking simulation study as a trial pilot test for its application on the human beings in the future.

## Materials and Methods

### Preparation of CAE

Methanolic extract of *Cicer arietinum* was prepared according to the method adopted by Marzouk et al. (20). One gram of finely *Cicer arietinum* seeds powder was mixed with 4 ml of methanol, heated at 60°C for 1 h while being shaken in a water bath. The resulting extract was centrifuged at 10000 rpm, 5 °C for 20 min. The resulting supernatant was filtered through filter paper (Whatman No. 1), concentrated on a rotary evaporator and dried by lyophilizer apparatus.

The percentage yield of the extract was calculated using the following formula:

$$\% \text{ Yield} = \frac{\text{Weight of the extract}}{\text{Weight of seed powder}} \times 100$$

$$\% \text{ Yield} = 15.833\%$$

The prepared CAE was stored in a desiccator until use.

### Amino acid analysis of CAE

The CAE was analyzed for amino acid content by acid hydrolysis method using the Automatic Amino Acid Analyzer (AAA 400, INGOS Ltd.) according to the method described by Block et al. (21). The dried ground sample of CAE (100 mg) was hydrolyzed with 6 N HCl (10 ml) in a sealed tube at 110°C in an oven for 24 h. After hydrolysis, the acid was evaporated to dryness under a vacuum of 80°C with the occasional addition of distilled water. The HCl free residue was dissolved in 2 ml loading buffer (6.2 M, pH 2.2) using a syringe.

## In silico study on human estrogen receptors

### Molecular modeling

Molecular modeling software SCIGRESS 3.0 (22) installed on Dell Precision T3500 workstation and HADDOCK (23) web server were used to study the docking of estrogens (estriol and  $\beta$ -estradiol) and phytoestrogens (genistein, daidzein, formononetin and biochanin A) with both of the human ERs  $\alpha$  and  $\beta$ .

### Geometry optimization

The structures of the estrogens and phytoestrogens were sketched using the medicinal chemistry platform SCIGRESS tools and then geometry optimized using Molecular Mechanics force field (MM3 method). After this, the structures were further optimized using semi-empirical quantum mechanical Parameterization Method 6 (PM6). The optimized structures were then validated by calculating the Infrared vibrational spectra using the same method (PM6) to ensure the reality of the structures. Finally, structures are optimized quantum mechanically by Density Function Theory (DFT) using the B3LYP functional followed by IR calculation using the same basis set. At this point, estrogen and phytoestrogen structures were ready for our study.

### Quantitative Structure-Activity Relationships (QSAR) parameters calculation

QSAR study was done (using SCIGRESS) to compare the activity and stability of the studied compounds with the standard estrogens. The parameters were calculated for the geometry-optimized structures. The QSAR parameters that used in this study included conformation minimum energy (Kcal/mol), total energy (Kcal/mol), heat of formation (Kcal/mol), dipole moment (Debye), ionization potential (eV), Log P, molar refractivity, polarizability ( $\text{\AA}^3$ ), solvent accessible surface area ( $\text{\AA}^2$ ) and the frontier energy gap (LUMO-HOMO) (eV).

### Molecular docking

Using experimentally solved structures of both human ER  $\alpha$  and  $\beta$ , we made our docking study. The protein data bank files 2Q70, 2QA8, 3Q95 and 3UUD re-

presenting human ER $\alpha$  and 1L2J, 1QKM, 1X7J as well as 3OLS representing human ER $\beta$  were downloaded from the protein data bank (www.pdb.org) (24) for using in our docking study. We made some modifications to the coordination files as a preparatory step for docking. We get the coordinates of one polypeptide chain from each of the downloaded PDB files (if it has more than one chain) and removed ligands using PyMOL software (25). In addition, *Rattus norvegicus* ER $\beta$  structure (PDB ID: 1QKN) is downloaded for testing against phytoestrogens. Due to the lack of rat ER $\alpha$  solved structures in the protein data bank, we built 3D structure model from its amino acid sequence using comparative protein modeling (26).

HADDOCK web server was used to perform molecular docking in this study. The easy interface was used in which the required files were the PDB of both protein and ligand and the active amino acids that take part in the interaction. These amino acids are retrieved from solved structures for both human ER $\alpha$  and ER  $\beta$ . Easy mode is used because we only have the amino acids that take part in the interaction with estrogens which we get from the solved structures (previously mentioned PDB files).

At the same time, we do the docking study with different software based on vina scoring function, AutoDock Vina (27). From HADDOCK and AutoDock Vina; docking scores of estrogens and phytoestrogens were retrieved and the docking poses were taken for comparison using PyMOL software.

### Animals

Thirty female 3-4 month-old Wistar albino rats (*Rattus norvegicus*) were purchased from the animal house of the National Research Center (NRC), Egypt. Rats were housed in polypropylene cages in an air-conditioned room at a temperature of  $23 \pm 2$  °C and under natural day and night cycle. They were fed standard chow pellets and drinking water *ad libitum*. The rats were acclimated for one week prior the commencement of the experiment.

### Ethical considerations

This study was carried out in strict accordance with the recommendations in the Guide for the Care and Use of Laboratory Animals, 8th edition. The experimental animal facility and protocol were approved by the Institutional Animal Care and Use Committee (IACUC) (CUFS/F/PHY/03/13) of the Faculty of Science, Cairo University, Egypt. All efforts were made to minimize suffering the surgery.

### Osteoporosis induction

Bilateral ovariectomy is a scientifically accepted model of osteoporosis and it was performed as described previously by Sayed et al. (28). The sham-operated group was handled as the ovariectomized (OVX) group, but the ovaries still intact.

### Grouping and treatment

Twenty four rats were randomized into four groups of 6 animals each as shown in figure 1. Surgery initiated at week 0 and the experiment was terminated at week 10. At the end of treatment period, the rats were eutha-

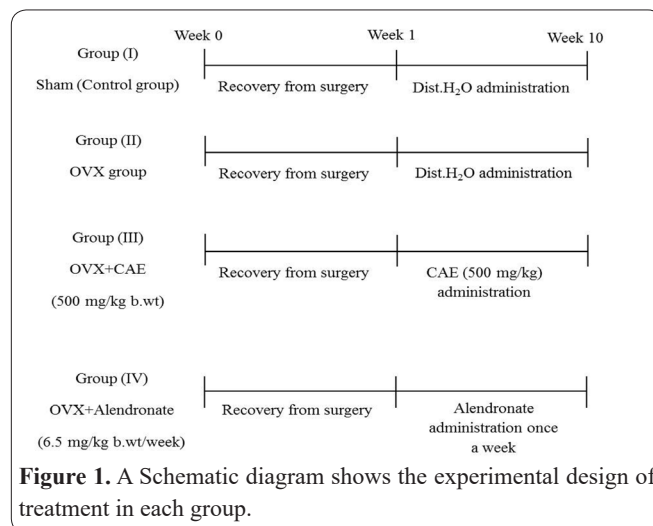


**Figure 1.** A Schematic diagram shows the experimental design of treatment in each group.

nized and the serum was then prepared by centrifugation of the collected blood (3000 rpm for 20 min.) and stored at -80 °C for estrogen (E2) analysis. The left femur was dissected from each animal and cleaned of all soft tissue, then washed in cold saline and homogenized with 0.1 M Tris-HCl buffer (pH 7.2), and stored at -80 °C for further analysis. The right femur bone was also carefully removed, cleaned and prepared for cortical bone histological examination to investigate microarchitectural changes. The uterus of each rat was also dissected, separated from the surrounding adipose and connective tissues and prepared for histological examination.

### Serum estrogen (E2) assay

The serum E2 level was determined by a radioimmunoassay (RIA) kit (DRG Diagnostics, Marburg-Lahn, Germany).

### Bone biochemical markers

Bone biochemical markers of OPG, RANKL and TRAP5b were measured in bone homogenate using an ELISA reader. Further, the ratio of OPG/RANKL was calculated to determine the net bone formation. The ratio was calculated after converting the serum RANKL (pmol/g tissue) to ng/g tissue to unify the unit.

### Uterine histological and morphometric examination

Routine histological processes were employed which includes paraffin inclusion, sectioning and hematoxylin-eosin staining. For morphometric measurements of the uterus, an image analyzer (Leica, QWIN version 3) coupled with a light microscope and the personal computer was used. The uterine morphometrical measurements include; the number of uterine glands, the thickness of the endometrium and myometrium.

### Cortical bone histological examination

The right femoral bone was removed and fixed in 10% neutral buffered formalin for 48 h and decalcified in 10% EDTA (pH 7.4) at 4 °C for 4 weeks. After decalcification, each bone sample was embedded in paraffin blocks in a routine manner and cut longitudinally into 5 $\mu$ m sections. Then cortical sections were stained with hematoxylin and eosin.

### Statistical analysis

Results of the present study were expressed as

mean±SEM. Data were analyzed by one way ANOVA using the Statistical Package for the Social Sciences (SPSS) program, version 15 (SPSS Institute, Inc., Chicago, IL, USA) followed by Duncan test to compare significance between groups. The difference was considered significant when P value less than 0.05 (P<0.05).

**Results**

**Amino acid content of CAE**

The amino acid profile of the present study indicates that the CAE is an excellent source of essential and non-essential amino acids (Table 1). CAE contains a higher concentration of non-essential amino acids, where the levels of glutamic acid and arginine are remarkably higher than any other amino acid species (Fig. 2). The present extract (CAE) provides a valuable addition to the nutrient database of amino acid; consequently CAE may be used as amino acid complement without any loss of essential nutrient value.

**CAE enhance bone turnover markers and retained the bone structure of OVX rats**

The present study revealed that ovariectomy induces E2 deficiency and hence affect some bone remodeling markers. Bone OPG and OPG/RANKL ratio were observed in untreated OVX group relative to sham control group. As shown in table 2, significant elevation of bone RANKL and TRAP5b levels were observed in OVX rats compared to sham. CAE enhance E2, OPG and OPG/RANKL levels as well as suppress RANKL and TRAP5b concentrations. In addition, alendronate improved the bone turnover markers significantly but no change in TRAP5b level was observed.

Histological examination of cortical bone of OVX rats revealed a thinning cortical bone and a dispersion of many resorption pits in the cortex in comparison with sham one (Fig. 3). OVX rats treated with CAE had thicker cortical bone and no visible resorption pits when compared with untreated OVX rats. Further, the cortical bone of alendronate-treated group was apparently similar to that of the control group.

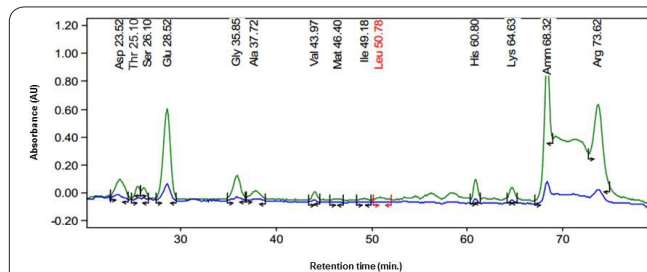


**Figure 2.** HPLC chromatogram of CAE.

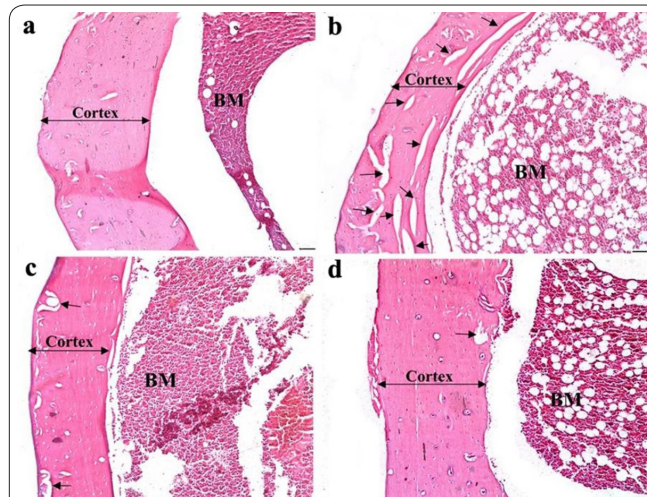


**Figure 3.** Photomicrographs of the cortical bone architecture of the different groups. (a) Sham group showing normal cortical bone thickness, (b) OVX group showing marked decrease in the thickness of cortical bone and wide resorption pits, (c) CAE -treated OVX rats showing nearly normal cortical thickness with no resorption pits, (d) Alendronate-treated OVX rats showing more or less the normal cortical structure. BM: bone marrow; arrows point to resorption pits. H&E staining; Scale bar = 100µm.

**Morphological analyses of uterus**

As shown in figure 4, ovariectomy resulted in atrophy of the uterus. Since a minimal number of glands in addition to a dramatic decrease in endometrium and myometrium thickness were observed compared with sham control uterus. CAE slightly maintain uterine structure more or less at the level of sham rats, where

**Table 1.** Amino acids content of CAE.

Essential amino acids	Value (g/100 g)	Non-essential amino acids	Value (g/100 g)
Histidine	0.7656	Alanine	0.594
Luicine& isoleucine	0.310	Arginine	5.06
Lysine	0.464	Aspartic acid	1.412
Methionine	0.073	Glutamic acid	6.318
Valine	0.3256	Glycine	1.54
Threonine	0.2596	Serine	0.198

**Table 2.** Effect of CAE on bone formation/resorption markers of OVX rats.

Parameter	Sham	Vehicle	OVX	
			CAE	Alendronate
E2 (pg/ml)	57.250±0.250 <sup>a</sup>	46.300±0.413 <sup>b</sup>	56.750±1.060 <sup>a</sup>	58.6400±0.519 <sup>a</sup>
OPG (ng/g.tissue)	34.062±2.843 <sup>a</sup>	22.103±1.444 <sup>b</sup>	27.416±1.158 <sup>bc</sup>	31.738±2.544 <sup>ac</sup>
RANKL (pmol/g.tissue)	11.669±0.997 <sup>a</sup>	18.803±2.787 <sup>b</sup>	12.722±1.478 <sup>a</sup>	9.285±1.675 <sup>a</sup>
OPG/RANKL ratio	3.944±0.639 <sup>ac</sup>	1.5±0.264 <sup>b</sup>	2.963±0.454 <sup>bc</sup>	4.946±0.835 <sup>a</sup>
TRAP5b (pg/g.tissue)	55.805±2.996 <sup>a</sup>	69.083±4.295 <sup>b</sup>	61.666±4.519 <sup>ab</sup>	79.391±1.794 <sup>c</sup>

Values are mean ± SEM (n=6). Values with different superscript letters are significantly different (p < 0.05). Data were analyzed by ANOVA post hoc with Duncan test.

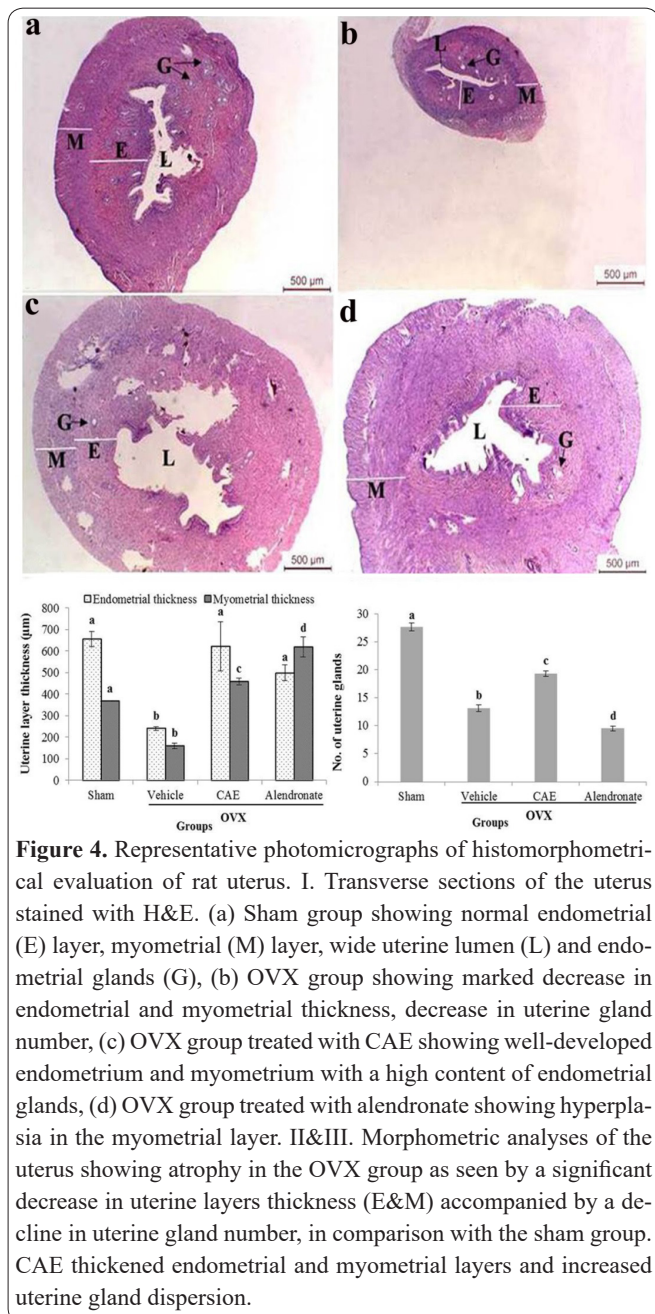


**Figure 4.** Representative photomicrographs of histomorphometrical evaluation of rat uterus. I. Transverse sections of the uterus stained with H&E. (a) Sham group showing normal endometrial (E) layer, myometrial (M) layer, wide uterine lumen (L) and endometrial glands (G), (b) OVX group showing marked decrease in endometrial and myometrial thickness, decrease in uterine gland number, (c) OVX group treated with CAE showing well-developed endometrium and myometrium with a high content of endometrial glands, (d) OVX group treated with alendronate showing hyperplasia in the myometrial layer. II&III. Morphometric analyses of the uterus showing atrophy in the OVX group as seen by a significant decrease in uterine layers thickness (E&M) accompanied by a decline in uterine gland number, in comparison with the sham group. CAE thickened endometrial and myometrial layers and increased uterine gland dispersion.

it can proliferate the uterine endometrium, increased endometrial and myometrial thickness, and endometrial glands numbers. Alendronate treatment to OVX rats increased the abovementioned indices of the uterus. Additionally, the uterine structure becomes hypertrophic and hyperplastic following alendronate.

### Quantitative Structure-Activity Relationships (QSAR)

Table 3 shows the calculated values of some Quantitative Structure-Activity Relationships (QSAR) parameters. These values are calculated using semi-empirical quantum mechanical parameterization method PM6 for the optimized structures of both estrogens (estriol and  $\beta$ -estradiol) and the phytoestrogens (genistein, daidzein, formononetin and biochanin A). Table 3 shows some parameters that reflect the stability of a structure (conformational minimum energy, dielectric energy, steric energy, total energy and heat of formation) and other parameters that reflect the reactivity of the structure [dipole moment, electron affinity, molar refractivity, the frontier energy gap (LUMO-HOMO), io-

nization potential, Log P, molecular weight and solvent accessible surface area].

From the first five columns of table 3 (that reflect structural stability), we can found that genistein, biochanin A and estriol, have the most stable conformations compared to other compounds. They have the lowest conformation minimum energies (-152.961, -148.82 and -146.127 Kcal/mol, respectively), lowest total energies (-94832.248, -99323.194 and -97642.209 Kcal/mol, respectively) and the lowest heat of formations (-170.392, -165.151 and -161.335 Kcal/mol, respectively). Also, genistein and biochanin A has the lowest steric energy (2.352 and 2.387 Kcal/mol, respectively). On the other hand, the dielectric energy of the estrogens is higher than the phytoestrogens. From the remaining columns of table 3 (that reflect structural reactivity), we found that the estrogens have lower dipole moment compared to the phytoestrogens. This implies higher reactivity compared to estrogens. This is supported by the better values of the ionization potentials, Log P values, frontier energy gaps (LUMO-HOMO), molar refractivity values and electron affinities of phytoestrogens compared to estrogens. On the other hand, the estrogens and biochanin A have higher solvent accessible surface areas. This may be in part due to their higher molecular weights compared to the other compounds under our study.

### Molecular docking

Rat estrogen receptors  $\alpha$  and  $\beta$  are used to test the binding ability of phytoestrogens and compare it to estrogens. Rat ER $\beta$  has solved structure in the protein data bank while rat ER $\alpha$  still not solved experimentally. Phyre2 webserver was used to build a 3D structure for rat ER $\alpha$  from its sequence (GenBank: BAI48013.1) using human estrogen receptor  $\alpha$  ligand binding domain (PDB ID: 1XPC) as a homolog (sequence Identity 97%). The model is valid based on Ramachandran plot (29) (94.5% in the most favored region and only 0.8% in the disallowed region), ERRAT (30) (overall quality factor 87.391%) and Verify 3D (31) (83.19% of the residues had an averaged 3D-1D score  $\geq 0.2$ ). On the other hand, rat ER $\beta$  solved structure (PDB ID: 1QKN) is used in this docking study. AutoDock Vina is used to testing the binding affinity of both estrogens and phytoestrogens to the rat ER $\alpha$  (model) and rat ER $\beta$  solved structure. For rat ER $\alpha$ , A41, L82, K92 and G212 are used as flexible during the docking calculations. On the other hand, S252 and E344 were used as flexible during the docking in the case of rat ER $\beta$ .

In order to identify the active amino acids of the human ER $\alpha$  and  $\beta$ , this study used the solved structures of human ER with ligands have the same properties of our tested compounds. A collection of ER $\alpha$  structure files (PDB code: 1AS2, 1ERE, 1G50, 1GWR, 1QKU, 1X7R, 2OCF, 2QA8, 3Q95, 3UUD and 4PXM) are studied for their ligand interactions. The ligand in 3Q95 is estriol and in 1X7R and 2QA8 it is genistein while the rest of structures estradiol is the ligand. For human ER $\beta$ , we studied the structures of 3OLL, 3OLS, 1QKM and 1X7J. The amino acids that take part in the interaction with ligands were E353, R394, F404 and H524 for ER $\alpha$  while for ER $\beta$  E305, R346, F356 and H475 were the interacting residues. These active amino acids are utilized by HADDOCK web server and AutoDock Vina for the

**Table 3.** Quantitative Structure-Activity Relationship (QSAR) parameters calculated for both estrogens and phytoestrogens using semi-empirical Parameterization Method 6 (PM6). The best values are in bold as illustrated in the text.

Compound	Conformation minimum energy [kcal/mol]	Energy dielectric [kcal/mol]	Energy steric [kcal/mol]	Energy total [kcal/mol]	Heat of formation [kcal/mol]	Dipole moment [debye]	Electron affinity [eV]	(LUMO–HOMO) energy gap [eV]	Ionization potential [eV]	Log P	Molar refractivity	Molecular weight [mass_au]	Solvent accessible surface area [A^2]
<i>Estriol</i>	<b>-146.127</b>	-0.752	60.463	<b>-97642.209</b>	<b>-161.335</b>	4.685	-0.239	8.987	-8.964	3.24	80.979	<b>288.381</b>	<b>299.395</b>
<i>β-Estradiol</i>	-101.397	-0.561	48.735	-90028.201	-112.673	3.838	-0.283	9.001	-8.966	4.01	79.618	<b>272.382</b>	<b>285.567</b>
<i>Genistein</i>	<b>-152.961</b>	<b>-0.941</b>	<b>2.352</b>	<b>-94832.248</b>	<b>-170.392</b>	<b>8.453</b>	<b>0.967</b>	<b>8.097</b>	<b>-9.146</b>	<b>1.96</b>	<b>70.823</b>	270.237	271.457
<i>Daidzein</i>	-99.265	<b>-0.988</b>	<b>6.75</b>	-87181.062	-117.071	<b>8.224</b>	<b>0.846</b>	<b>8.11</b>	<b>-9.11</b>	<b>2.25</b>	<b>69.128</b>	254.237	264.873
<i>Formononetin</i>	-95.091	<b>-0.936</b>	<b>6.705</b>	-91672.324	-111.777	<b>8.084</b>	<b>0.785</b>	<b>8.009</b>	<b>-9.008</b>	<b>2.28</b>	<b>73.898</b>	268.264	284.177
<i>Biochanin A</i>	<b>-148.82</b>	<b>-0.883</b>	<b>2.387</b>	<b>-99323.194</b>	<b>-165.151</b>	<b>8.543</b>	<b>0.884</b>	<b>8.001</b>	<b>-9.044</b>	<b>1.99</b>	<b>75.592</b>	<b>284.263</b>	<b>291.031</b>

**Table 4.** Amino acids involved in the interaction of estrogen and phytoestrogens with estrogen receptors  $\alpha$  and  $\beta$ . The interaction is mediated by either H-bond formation (between the small molecules and the mentioned amino acids) or  $\pi$  staking (between aromatic rings found in the structures of all estrogens and phytoestrogen and aromatic amino acids H, F, W and Y). The docking study was done with AutoDock Vina software and the data mining performed by PyMOL software. Star (\*) indicate H-bond formed between the small molecules and water in the vicinity of the binding site.

origin	Protein	PDB code	Estrogens			Phytoestrogens			
			$\beta$ -estradiol	Estriol	Genistein	Diadzein	Formononetin	Biochanin A	
Rat	ER $\beta$	1QKN	Y366 and N425	Y366 and N425 *	Y366 and N425	Y366 *	Y366	S288 and Y366	
Rat	ER $\alpha$	Model	F407, F428 and H527	F407 and H527	W386, F407 and F428	W386, F407 and F428	W386, F407, F428 and H527	T350, W386, F407 and F428	
Human	ER $\alpha$	2QA8	F404	F404	R394, F404 and H524	R394 and F404	L387, R394, F404 and H524	L346, R394, F404 and H524	
Human	ER $\alpha$	3Q95	P365	V376 and E380	E419, H550 and P552	K362 and P365	D374, H377 and A546	H516	
Human	ER $\alpha$	3UUD	E542	R434 and H513	H476 and Y459	T431 and H513	H516 *	E470 and H474	
Human	ER $\beta$	3OLS	F356, F377 and H425	H428 *	P317 and H428	P412	S323, P412 and L413	R329, S409 and Y411	
Human	ER $\beta$	1X7J	E305, R346 and F356 *	K314 and E493	E305, R346, F356, F377 and H475 *	F319	V320 and E493	L298, L339, R346, F356 and H475 *	
Human	ER $\beta$	1QKM	W335 and Y488	H350 and P358	L339, R346, F356 and H475 *	E305, R346 and F356	E276, H279, W345 and P358	P317 and H428 *	

docking study. The present study used these four amino acids for each of the human ER $\alpha$  (PDB codes: 2Q70, 2QA8, 3Q95 and 3UUD) and  $\beta$  (PDB codes: 1L2J, 1QKM, 1X7J and 3OLS) as the active amino acids in HADDOCK easy interface and make our docking without using any restraint files. These amino acids are treated as flexible in AutoDock Vina using AutoDock Tools package (32).

Figures 5 a and 5 b show the docking scores obtained from HADDOCK web server for both estrogens and the phytoestrogens (Figure 5a represent the scores for human ER $\alpha$  complexes while figure 5b represent the scores for human ER $\beta$  complexes). The error bars are used because HADDOCK gather the complexes generated which have small Root Mean Square Deviation (RMSD) and represent it by a cluster. Figure 5 c shows the docking scores calculated by AutoDock Vina for human and rat ER $\alpha$  and ER $\beta$ . Our goal is to use phytoestrogen for human and this *in silico* study suggests the effectiveness of these molecules as good binders as estrogens. This can be obvious from docking scores values (binding affinities) and docking poses (protein/

ligands interactions) in figures 5 and 6, respectively.

In order to trust our docking study, we compared the solved structures of human ER $\alpha$  (2QA8) and  $\beta$  (1X7J) to the docking complexes we obtained using AutoDock Vina. Figure S1 shows the superposition of the solved (cyan/green for ER $\alpha$  and ER $\beta$ , respectively) and the calculated docked (magenta) genistein structures. Hydrogen atoms are missed in the solved structures because X-ray crystallography is the method used to solving the structures. It is obvious the correctness of our docking model since it coincides with the solved structure. Hence we can trust the docking experiment and now we need to know how the phytoestrogens bind to the estrogen receptors.

Some of the docking poses are shown in figure 6. This figure clarifies the interactions occurred between the ligands (both estrogens and phytoestrogens) and the human ER $\alpha$  (PDB ID 2QA8) and  $\beta$  (PDB ID 1X7J). Amino acids that take part in the interaction with the ligands are represented (lines) and labeled. These are listed in table 4 along with other structures used in this study. The main interaction types that predominate here is the ring stacking ( $\pi$ -stacking) and H-bonding. This is due to the chemistry of the estrogens and the phytoestrogens. Both have aromatic rings and hydroxyl groups that fit inside the aromatic-rich binding sites. The flexibility of four amino acids (based on different structures have different ligands) in each target protein made the

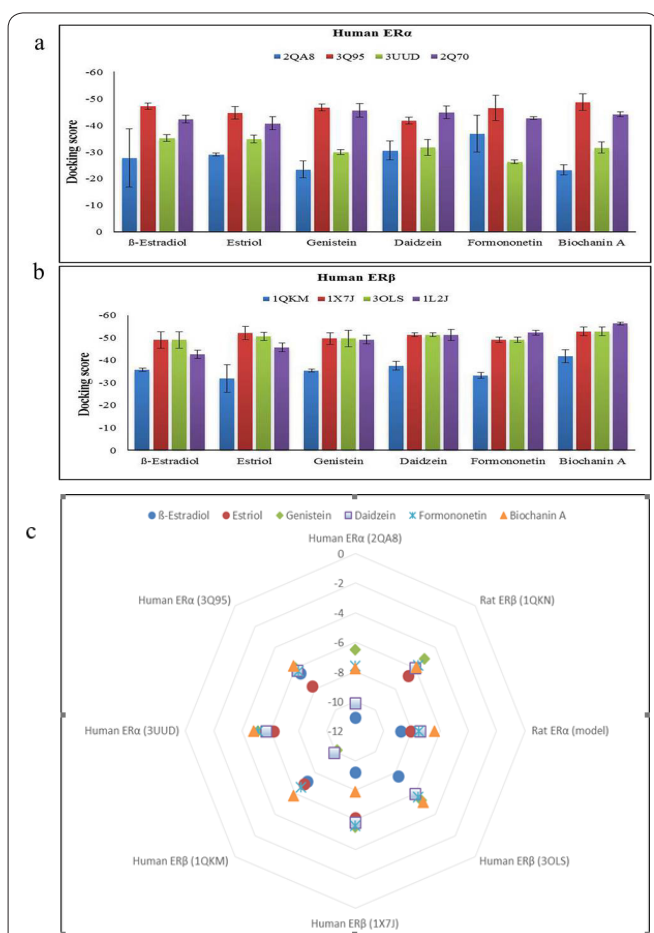


**Figure 5.** Bar graphs of the docking scores result from HADDOCK web server for the docking of both estrogens ( $\beta$ -estradiol and estriol) and phytoestrogens (genistein, daidzein, formononetin and biochanin A) with human ER $\alpha$  (a) and ER $\beta$  (b). The score of the best cluster recorded and represented by a column with error bars represent the cluster standard deviation (SD). 2QA8, 3Q95, 3UUD and 2Q70 represent human ER $\alpha$  while, 1QKM, 1X7J, 3OLS and 1L2J represent human ER $\beta$ . c) The docking scores (binding affinity in Kcal/mol) calculated using AutoDock Vina software. Rat and human ER  $\alpha$  and  $\beta$  are used as target proteins. Each ligand is represented by different colors as shapes as shown in the top of the figure.

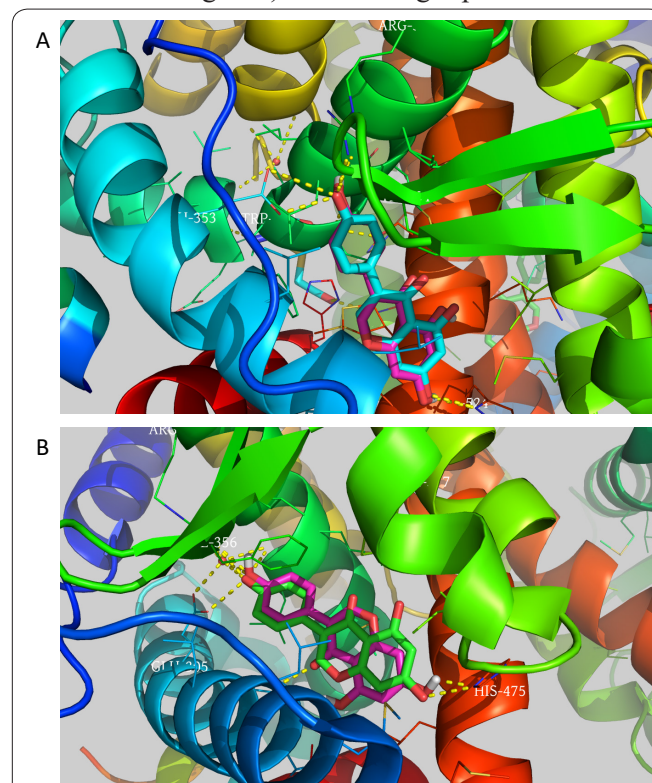


**Figure S1.** (A) Superposition of the docked genistein (magenta sticks) to human ER $\alpha$  (PDB ID: 2QA8) and the solved structure (that contains genistein (cyan sticks)). (B) Superposition of the docked genistein (magenta sticks) to human ER $\beta$  (PDB ID: 1X7J) and the solved structure (that contains genistein (green sticks)). A water molecule (red circle since hydrogens are not visible by x-rays) is taking part in the interaction at the binding site and facilitate the binding. It binds to both the ligand and the protein. In both figures, yellow dashed lines are the polar contacts that may be H-bonds formed between the ligand and the binding site of the protein.

docking flexible and more amino acids are suitable to interact with the ligands as shown in table 4. In addition,

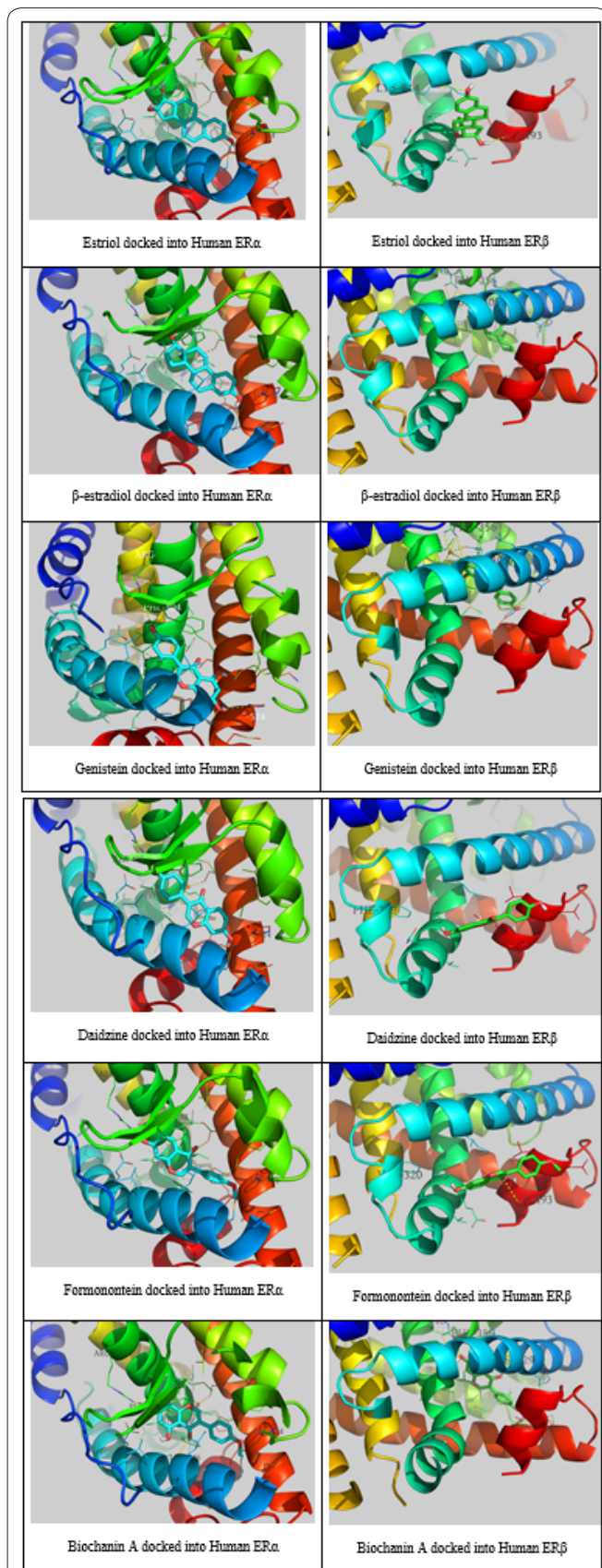


**Figure 6.** Docking poses for estrogens ( $\beta$ -estradiol and estriol) and phytoestrogens (genistein, daidzein, formononetin and biochanin A) with both human ER  $\alpha$  (PDB ID: 2QA8) and  $\beta$  (PDB ID: 1X7J). Ligand site representation by PyMOL is used to construct the images. The ligands (estrogen and phytoestrogen) are represented as sticks while the protein is cartoon represented with some labels and lines which refer to amino acid side chains that are involved in the interaction with the ligands.

for human and rat ER $\beta$ , water molecules are found in the binding site forming H-bonds with both the ligands and the protein. This facilitated binding is reflected in the binding mode of ER $\beta$  (see Table 4 and figure 6).

The main interacting amino acids are mostly the same amino acids recorded from the PDB files which are: E353, R394, F404 and H524 for human ER $\alpha$  and E305, R346, F356 and H475 for human ER $\beta$ . Some amino acids also involved in the binding but not recorded in the PDB files (table 4). This is due to the flexibility in our docking experiment and the water molecules found in some solved structures of ER $\beta$ . Since the chemical structures of the phytoestrogens is similar to that of estrogens (see figure S2), which consists mainly from aromatic rings and hydroxyl group, the interaction with ER is suggested to be the same with some minimal differences that slightly affect the binding. It is apparent from both figures 5 and 6 that there is no significant difference between the docking scores and poses for both estrogens and phytoestrogens. This implies the ability of phytoestrogens to bind to ER active site similar to normal estrogens. This suggests the possible compensatory effect of phytoestrogen in case of estrogen deficiency.

## Discussion

Postmenopausal osteoporosis originated from the cessation of ovarian hormones at menopause which prolongs bone loss. Phytoestrogen and essential amino acids are proven to modulate the growth and the differentiation of osteoblasts and possessing anti-osteoporotic effects (33, 34). Therefore, the main goal of this study is to find natural treatment gathered these two properties. *Cicer arietinum* is known for its higher proteinous and phytoestrogen contents (13-15). Thus, the present investigation attempt to study the dual action of both

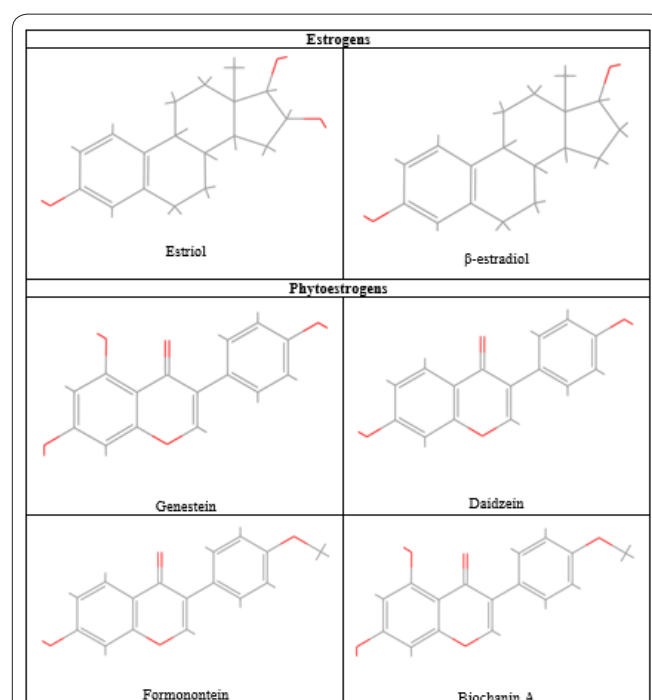


**Figure S2.** Two-dimensions structures of the estrogen and phytoestrogens used in the docking experiment showing the structural similarities. Maestro software is used to represent the structures in which Oxygen is represented in red while Carbon and Hydrogen are in gray

phytoestrogen and amino acids contents of *Cicer arietinum* extract (CAE) and the possible *in silico* and *in vivo* mechanisms behind these effects using ovariectomized (OVX) rats as a model of postmenopausal osteoporosis.

The present study revealed that ovariectomy resulted in estrogen depletion which manifested by a significant decrease in the E2 level relative to sham level in addition to the atrophy of the uterus. This is matching with the report of Diel et al. (35), who disclosed that the uterotrophic assay expresses the estrogenic activity *in vivo*. The present study evidenced the uterus atrophy histologically, as the uterus of OVX group show marked decrease in the thickness of endometrial and myometrial, a decrease in number of uterine gland. This result is parallel with the result of Koo et al. (36).

Furthermore, the present work revealed that ovariectomy elevates the bone TRAP5b concentration significantly which reflects the severity of bone resorption in OVX group. Omi and Ezawa (37) mentioned that ovariectomy resulting in an increase in bone resorption. The present study attributes this to the RANK/RANKL/OPG signaling pathway. Estrogen deficiency up-regulate the production of RANKL; which is one of the responsible cytokines that enhanced osteoclastogenesis and consequently bone loss (38). Thus, the present study interprets the increased TRAP5b level of OVX rats to estrogen deficiency (manifested in the present study) that in turn stimulate the osteoblast to produce RANKL (which increased in the present study). The latter accelerated osteoclast differentiation and bone loss. This emphasized the pronounced decreased level of OPG, where estrogen deficiency provokes osteoclastogenesis by down-regulating OPG and consequently suppress the OPG/RANKL ratio. Thus, facilitating the binding of RANKL to RANK receptor and hence activate osteoclast differentiation. The increased bone TRAP5b activity and RANKL simultaneously with the decrease of OPG/RANKL ratio matching with cortical thinning and porosity. This finding is consistent with Fahmy et al. (13) and Sirasanagandla (39), who found that ovariectomy increased the serum RANKL and TRAP5b and decline the serum OPG levels.

The physiological and morphological alterations induced by ovariectomy were recovered by administration of CAE, as most of the marker levels become almost similar to sham marker levels. CAE resulted in an increase in the E2 level of the OVX group significantly. This shown through restoring the lining of the uterus of the CAE-treated rats to the sham group. This indicates that CAE has a direct estrogenic activity on the uterus. The present study attributes this ability to the phytoestrogen contents of CAE. Where, docking study revealed that genistein, daidzein, formononetin and biochanin A can bind effectively with ER $\alpha$  which is predominantly expressed on the uterus and localized in the nuclei of the uterine glands (40, 41). This explains that CAE phytoestrogen compounds can act as endogenous estrogen by binding to its receptor binding site. The high docking scores (calculated by HADDOCK and AutoDock Vina) of the CAE phytoestrogen compounds signifies that they can bind to the ERs binding site with a strong binding affinity more or less similar to the standard estradiol and  $\beta$ -estradiol. In addition, the interaction pattern of standard estrogens is maintained in phytoestrogens.

Therefore, phytoestrogens can prevent uterus atrophy induced by estrogen deprivation. This explanation is in harmony with Santell et al. (42), who reported that genistein binds with ER $\alpha$  to improve uterine status.

The increased E2 in the OVX-CAE treated group evoke an increase in the OPG and diminish the RANKL levels. This manifested by the pronounced increase in the OPG/RANKL ratio. Thus, the present study assumed that CAE has the potency to block osteoclastogenesis, since, OPG/RANKL ratio reflect the osteoformation/osteoresorption (43). CAE may stimulate osteoblastic cells to up-regulate the secretion of OPG which binds with RANKL; consequently reduce the RANK/RANKL interaction and hence inhibit osteoclastogenesis. The up-regulation of OPG in the CAE group may be due to its phytoestrogen contents which mimic the action of estrogen in up-regulating the OPG normally, and this proved by binding of phytoestrogen contents of CAE with ERs  $\alpha$  and  $\beta$ . Albertazzi (44) revealed that genistein binds with ER $\beta$  to prevent bone loss. Interestingly, not only the phytoestrogen contents of the CAE participating in the modulation of bone loss; but also its amino acids contents contributing to bone protection and/or bone loss modulation. Recently, it was reported that some of the non-essential amino acids including alanine, arginine, glutamic acid, leucine, lysine and glycine (present in the CAE) play a major role in bone health as they promote osteoblast growth and differentiation (45). Further, CAE contains a remarkable concentration of arginine which is a key building block to repair the damaged bone and consequently enhance osteoblastogenesis (33, 46). Goel et al. (47) and Vijayan et al. (48) added that L-arginine and methionine, that existing in the CAE, attenuate bone loss through inhibition of osteoclast. This indicates that CAE may exert positive effects on bone formation which confirmed by increased thickness of the cortical bone, besides its osteoclastogenesis inhibition which affirmed through the decreased level of TRAP5b and lack of porosity in the cortical bone.

In conclusion, CAE has an estrogenic-like activity and is a potent inhibitor of osteoclastogenesis. These effects may be due to its phytoestrogens in combination with its bone-protective amino acids. Thus, CAE confirmed its efficacy in a pre-clinical study but future studies will be needed to evaluate its clinical efficacy for the treatment of osteoporosis in postmenopausal women.

### Acknowledgements

We thank colleagues of the Cairo University Research Park for imaging the histological photos. Thanks to Prof. Dr. Wael Elshemey for performing some of the calculations using his own computational Facility.

### Conflict of interest

The authors declare no conflicts of interest.

### Author Contributions

Amany A. Sayed conceived, designed the experiments and performed the biological experiments. Abdo A. Elfiky carried out the computational work including QSAR, molecular modeling and docking. All authors have contributed to the interpretation of results and the writing of the manuscript.

## References

- Shah A, Kolhapure SA. Evaluation of efficacy and safety of Reosto in senile osteoporosis: A randomized, double-blind placebo-controlled clinical trial. *Indian Journal of Clinical Practice* 2004; 15(3): 25–36.
- Fraser LA, Vogt KN, Adachi JD, Thabane L. Fracture risk associated with continuation versus discontinuation of bisphosphonates after 5 years of therapy in patients with primary osteoporosis: a systematic review and meta-analysis. *Ther Clin Risk Manag* 2011; 7: 157–166.
- Lacey DL, Timms E, Tan HL, Kelley MJ, Dunstan CR, Burgess T, Elliott R, Colombero A, Elliott G, Scully S, Hsu H, Sullivan J, Hawkins N, Davy E, Capparelli C, Eli A, Qian YX, Kaufman S, Sarosi I, Shalhoub V, Senaldi G, Guo J, Delaney J, Boyle WJ. Osteoprotegerin ligand is a cytokine that regulates osteoclast differentiation and activation. *Cell* 1998; 93: 165–176.
- Ohwada R, Hotta M, Sato K, Shibasaki T, Takano K. The relationship between serum levels of estradiol and osteoprotegerin in patients with anorexia nervosa. *Endocrine Journal* 2007; 54(6): 953–959.
- Hofbauer LC, Dunstan CR, Spelsberg TC, Riggs BL, Khosla S. Osteoprotegerin production by human osteoblast lineage cells is stimulated by vitamin D, bone morphogenetic protein-2, and cytokines. *Biochem Biophys Res Commun* 1998; 250: 776–786.
- Luvizuto ER, Queiroz TP, Dias SMD, Okamoto T, Dornelles RCM. Histomorphometric analysis and immunolocalization of RANKL and OPG during the alveolar healing process in female ovariectomized rats treated with oestrogen or raloxifene. *Arch Oral Biol* 2010; 55: 52–59.
- Rogers A, Eastell R. Circulating osteoprotegerin and receptor activator for nuclear factor kappa B ligand: clinical utility in metabolic bone disease assessment. *J Clin Endocrinol Metab* 2005; 90(11): 6323–6331.
- Tanaka S, Nakamura K, Takahashi N, Suda T. Role of RANKL in physiological and pathological bone resorption and therapeutics targeting the RANKL-RANK signaling system. *Immunological Reviews* 2005; 208: 30–49.
- Bonjour JP. Protein intake and bone health. *Int J Vitam Nutr Res* 2011; 81: 134–142.
- Conconi MT, Tommasini S, Muratori E, Parnigotto PP. Essential amino acids increase the growth and alkaline phosphatase activity in osteoblasts cultured in vitro. *Farmaco* 2001; 56: 755–761.
- Beasley JM, Ichikawa LE, Ange BA, Spangler L, LaCroix AZ, Ott SM, Scholes D. Is protein intake associated with bone mineral density in young women?. *Am J Clin Nutr* 2010; 91(5): 1311–1316.
- Hu T, Rianon NJ, Nettleton JA, Hyder JA, He J, Steffen LM, Jacobs DR, Criqui MH, Bazzano LA. Protein intake and lumbar bone density: the Multi-Ethnic Study of Atherosclerosis (MESA). *Br J Nutr* 2014; 112(8): 1384–1392.
- Fahmy SR, Soliman AM, Sayed AA, Marzouk M. Possible antiosteoporotic mechanism of *Cicer arietinum* extract in ovariectomized rats. *Int J Clin Exp Pathol* 2015; 8(4): 3477–3490.
- Sánchez-Vioque R, Clemente A, Vioque J, Bautista J, Millán F: Protein isolates from chickpea (*Cicer arietinum* L.): chemical composition, functional properties and protein characterization. *Food Chemistry* 1999; 64: 237–243.
- Yust MM, Pedroche J, Giron-Calle J. Production of ace inhibitory peptides by digestion of chickpea legumin with alcalase. *Food Chemistry* 2003; 81: 363–369.
- Ibrahim M, Saleh NA, Jameel A, Elshemey WM, Elsayed AA. Structural and electronic properties of new fullerene derivatives and their possible application as HIV-1 protease inhibitors. *Spectrochim Acta A Mol Biomol Spectrosc* 2010; 75: 702–709.
- Talele TT, Arora P, Kulkarni SS, Patel MR, Singh S. Structure-based virtual screening, synthesis and SAR of novel inhibitors of hepatitis C virus NS5B polymerase. *Bioorganic & Medicinal Chemistry* 2010; 18: 4630–4638.
- Ibrahim M, Saleh NA, Elshemey WM, Elsayed AA. Hexapeptide functionality of cellulose as NS3 protease inhibitors. *Medicinal Chemistry* 2012; 8: 6–10.
- Elfiky AA, Elshemey WM, Gawad WA, Desoky OS. Molecular modeling comparison of the performance of NS5b polymerase inhibitor (PSI-7977) on prevalent HCV genotypes. *Protein Journal* 2013; 32(1): 75–80.
- Marzouk M, Soliman AM, Fahmy SR, Sayed AA. Ameliorative effects of *Cicer arietinum* extract and *Coelatura aegyptiaca* shell powder on estrogen sensitive organs in ovariectomized rats. *World Applied Sciences Journal* 2014; 31 (5): 863–872.
- Block RJ, Durrum EL, Zweig G. A manual of paper chromatography and paper electrophoresis. Academic Press; New York, 1958.
- Elfiky AA. Zika viral polymerase inhibition using anti-HCV drugs both in market and under clinical trials. *J Med Virol*. 2016;88(12):2044-2051.
- de Vries SJ, van Dijk M, Bonvin AM. The HADDOCK web server for data-driven biomolecular docking. *Nat Protoc*. 2010;5(5):883-897.
- Burley SK, Berman HM, Christie C, Duarte JM, Feng Z, Westbrook J, Young J, Zardecki C. RCSB Protein Data Bank: Sustaining a living digital data resource that enables breakthroughs in scientific research and biomedical education. *Protein Sci*. 2018;27(1):316-330.
- The PyMOL Molecular Graphics System, Version 2.0 Schrödinger, LLC.
- Kelley LA, Sternberg MJ. Protein structure prediction on the Web: a case study using the Phyre server. *Nat Protoc*. 2009;4(3):363-371.
- Trott O, Olson AJ. AutoDock Vina: improving the speed and accuracy of docking with a new scoring function, efficient optimization and multithreading. *J Comput Chem*. 2010; 31(2): 455–461.
- Sayed AA, Soliman AM, Fahmy SR, Marzouk M. Antiosteoporotic effect of *Coelatura aegyptiaca* shell powder on ovariectomized rats. *African Journal of Pharmacy and Pharmacology* 2013; 7(34): 2406–2416.
- Laskowski RA1, Rullmannn JA, MacArthur MW, Kaptein R, Thornton JM. AQUA and PROCHECK-NMR: programs for checking the quality of protein structures solved by NMR. *J Biomol NMR*. 1996;8(4):477-486.
- Hoof RW, Vriend G, Sander C, Abola EE. Errors in protein structures. *Nature*. 1996 23;381(6580):272.
- Lüthy R, Bowie JU, Eisenberg D. Assessment of protein models with three-dimensional profiles. *Nature*. 1992;356(6364):83-85.
- Morris GM1, Huey R, Lindstrom W, Sanner MF, Belew RK, Goodsell DS, Olson AJ. AutoDock4 and AutoDockTools4: Automated docking with selective receptor flexibility. *J Comput Chem*. 2009 Dec;30(16):2785-2791.
- Ahmed HA, Hamza AH: Potential role of arginine, glutamine and taurine in ameliorating osteoporotic biomarkers in ovariectomized rats. *Report and Opinion* 2009; 1(6): 24–35.
- Wang X, He Y, Guo B, Tsang MC, Tu F, Dai Y, Yao Z, Zheng L, Xie X, Wang N, Yao X, Zhang G, Qin L. In vivo screening for anti-osteoporotic fraction from extract of herbal formula Xianling gubao in ovariectomized mice. *PLoS One* 2015; 10(2): e0118184.
- Diel P, Schulz T, Smolnikar K, Strunck E, Vollmer G, Michna H. Ability of xeno- and phytoestrogens to modulate expression of estrogen-sensitive genes in rat uterus: estrogenicity profiles and uterotrophic activity. *J Steroid Biochem Mol Biol* 2000; 73: 1–10.
- Koo HJ, Sohn EH, Kim YJ, Jang SA, Namkoong S, Chan Kang

- S. Effect of the combinatory mixture of *Rubus coreanus* Miquel and *Astragalus membranaceus* Bunge extracts on ovariectomy-induced osteoporosis in mice and anti-RANK signaling effect. *J Ethnopharmacol* 2014; 151: 951–959.
37. Omi N, Ezawa I. The effect of ovariectomy on bone metabolism in rats. *Bone* 1995; 17: 163S–168S.
38. Hotokezaka H, Sakai E, Ohara N, Hotokezaka Y, Gonzales C, Matsuo K, Fujimura Y, Yoshida N, Nakayama K. Molecular analysis of RANKL-independent cell fusion of osteoclast-like cells induced by TNF- $\alpha$ , lipopolysaccharide, or peptidoglycan. *J Cell Biochem* 2007; 101: 122–134.
39. Sirasanagandla SR, Pai KSR, Bhat KMR. Preventive role of *Emblica officinalis* and *Cissus quadrangularis* on bone loss in osteoporosis. *International Journal of Pharmacy and Pharmaceutical Sciences* 2013; 5 (4): 465–470.
40. Kummer V, Masková J, Èanderle J, Zralý Z, Neèa J, Machala, M. Estrogenic effects of silymarin in ovariectomized rats. *Vet Med - Czech* 2001; 46(1): 17–23.
41. Winuthayanon W, Piyachaturawat P, Suksamrarn A, Burns KA, Arao Y, Hewitt SC, Pedersen LC, Korach KS. The natural estrogenic compound diarylheptanoid (D3): *in vitro* mechanisms of action and *in vivo* uterine responses via estrogen receptor  $\alpha$ . *Environ Health Perspect* 2013; 121: 433–439.
42. Santell RC, Chang YCH, Nair MG, Helferich WG. Dietary genistein exerts estrogenic effects upon the uterus, mammary gland and the hypothalamic/pituitary axis in rats. *J Nutr* 1997; 127: 263–269.
43. Udomsuk L, Chatuphonprasert W, Monthakantirat O, Churikhit Y, Jarukamjorn K. Impact of *Pueraria candollei* var. *mirifica* and its potent phytoestrogen miroestrol on expression of bone-specific genes in ovariectomized mice. *Fitoterapia* 2012; 83: 1687–1692.
44. Albertazzi P. Purified phytoestrogens in postmenopausal bone health: is there a role for genistein?. *Climacteric* 2002; 5 (2): 190–196.
45. Jennings A, MacGregor A, Spector T, Cassidy A. Amino acid intakes are associated with bone mineral density and prevalence of low bone mass in women: evidence from Discordant Monozygotic Twins. *J Bone Miner Res* 2016; 31(2): 326–335.
46. Huh JE, Choi JY, Shin YO, Park DS, Kang JW, Nam D, Choi DY, Lee JD. Arginine enhances osteoblastogenesis and inhibits adipogenesis through the regulation of Wnt and NFATc signaling in human mesenchymal stem cells. *Int J Mol Sci* 2014; 15(7): 13010–1329.
47. Goel SC, Gyanendra Kumar JHA, Singh AK, Agarwal N, Singh TB, Manjhi B. Role of L-arginine in treatment of osteoporosis. *International Journal of Orthopaedics* 2014; 1(4): 177–180.
48. Vijayan V, Khandelwa M, Manglani K, Gupta S, Surolia A. Methionine down-regulates TLR4/MyD88/NF- $\kappa$ B signalling in osteoclast precursors to reduce bone loss during osteoporosis. *Br J Pharmacol* 2014; 171: 107–121.